NACA

RESEARCH MEMORANDUM

AN EXPERIMENTAL INVESTIGATION OF THE FLOW PHENOMENA OVER BODIES AT HIGH ANGLES OF ATTACK AT A MACH NUMBER OF 2.01

By John P. Gapcynski

Langley Aeronautical Laboratory
Langley Field, Va.

NATIONAL ADVISORY COMMITTEE
FOR AERONAUTICS

WASHINGTON

October 27, 1955

NATIONAL ADVISORY COMMITTEE FOR AERONAUTICS

RESEARCH MEMORANDUM

AN EXPERIMENTAL INVESTIGATION OF THE FLOW PHENOMENA OVER BODIES AT HIGH ANGLES OF ATTACK AT A MACH NUMBER OF 2.01

By John P. Gapcynski

SUMMARY

An investigation has been made in the Langley 4- by 4-foot supersonic pressure tunnel at a Mach number of 2.01 to study the wake patterns in the lee of bodies at high angles of attack. Two cylindrical body shapes, one circular and the other elliptical in cross section, were each tested with a fineness-ratio-3.5 ogival nose and a fineness-ratio-6 conical nose. In addition, the circular cylinder model was tested with a spike-tipped cone. The fineness ratio of the cylindrical portion of each model was 7. Static and instantaneous pressure measurements at two longitudinal body stations as well as vapor-screen photographs of the flow over the aft station were obtained for a range of angles of attack from 17° to 50°, for a Reynolds number of 3.46×10^6 per foot.

In general, as the angle of attack was increased the wake patterns in the lee of the bodies changed from a symmetrical pair of vortices to an asymmetrical distribution of two or more vortices. The angle at which an asymmetrical flow first appeared for any particular body shape was dependent upon the model nose configuration.

An unsteady asymmetrical configuration of vortices was not found to exist for any appreciable angle-of-attack range for the bodies used in this investigation. Although some vortex motion was apparent, a rapid aperiodic switching of the vortices was noted only for the spike-tipped circular cylinder model near an angle of 28°.

As the angle of attack was increased beyond 40°, the individual vortices in the lee of the conical-nosed circular and elliptical cylinder models appeared to lose strength and definition. These phenomena were not noted for the elliptical body with the major axis perpendicular to the cross flow.

INTRODUCTION

A knowledge of the flow phenomena about bodies at high angles of attack has become increasingly important of late due to the maneuverability requirements of supersonic missile and aircraft configurations. In addition, a thorough understanding of body wake characteristics and their effect on surfaces subject to wake interference is necessary since these factors may have some bearing on the losses in directional stability which are being encountered in present-day supersonic aircraft. Previous investigations (refs. 1 to 5) have shown that at supersonic speeds vortices are formed in the lee of bodies at angles of attack. These vortices, which extend downstream from the body nose section, were found to have the following characteristic patterns: a steady symmetric configuration of two vortices at low angles of attack, a steady asymmetric configuration of two or more vortices at moderate angles, and an unsteady configuration of two or more vortices at very large angles of attack. The angle at which any particular vortex pattern existed was found to be dependent upon the model geometry and the Reynolds number of the flow.

The present investigation was initiated in order to obtain a knowledge of the effect of these vortex patterns, in particular the unsteady patterns, on the aerodynamic characteristics of bodies at high angles of attack. In its original state, the program for this investigation consisted of tests, at a Mach number of 2.01, of two cylindrical bodies, one of circular cross section and the other of elliptical cross section. A fineness-ratio-3.5 ogival nose was used with each body and the angle-of-attack range was from 0° to 34.5°. Circumferential static as well as dynamic or instantaneous pressure measurements were to be obtained at two stations on the cylindrical portion of each body. However, preliminary vapor-screen tests showed that an unsteady flow condition could not be obtained with the ogive-cylinder bodies for the angle-of-attack range considered. Therefore, the program was expanded to include a fineness-ratio-6 conical nose for each body and a spike-tipped cone for the circular body. In addition, the maximum angle of attack was changed to 50°. Due to model mounting considerations, this necessitated a minimum angle of attack of 17°. These changes were based on the results given in reference 2. The Reynolds number of the majority of the tests was 3.46×10^6 per foot. It should be noted that an unsteady flow condition was not found to exist, and therefore no record of the instantaneous pressure variations have been presented.

SYMBOLS

ρ	mass density of air
V	airspeed
a	speed of sound in air
M	Mach number, V/a
α	angle of attack
q	dynamic pressure, $\frac{1}{2}\rho V^2$
p	static pressure (free stream)
p_l	local static pressure
P	pressure coefficient, $\frac{p_l - p}{q}$
θ	body polar angle measured counterclockwise in plane perpendicular to axis of body when facing downstream ($\theta = 0^o$ windward of body in plane of angle of attack)

MODELS AND TESTS

Sketches of the models are shown in figures 1(a) and 1(b). Two different cylindrical body shapes, with fineness ratios of approximately 7, were used. One of the body shapes was circular in cross section, and the other elliptical with a ratio of major to minor axes of 2. A fineness-ratio-3.5 ogival nose and a fineness-ratio-6 conical nose were available for each body shape. (For the elliptical body shape the fineness ratio was defined on the basis of the square root of the product of the major and minor axis.) In addition, a spike-tipped cone with an overall fineness ratio of 6 was used with the circular body. In order to facilitate identification, each test configuration will be referred to by the nose shape and the body cross-sectional shape. With reference to the elliptical model, it will also be necessary to specify the orientation of the major axis with respect to the cross flow.

Pressure measurements on the cylindrical portion of each body were obtained at two stations located 5 and 15 inches (2 and 6 body diameters

for the circular model) forward of the model base. At each station there were 36 static orifices located 10° apart. In addition, several electrical pressure pickups were located at each station as shown in figure 1(c).

Visual observation of the flow phenomena was made possible by means of the vapor-screen technique. Briefly, this technique involves the introduction of water into the airstream so that a fine fog is formed in the test section of the tunnel. A plane of light from a high intensity source is then projected across the test section at right angles to the tunnel axis. Flow disturbances are then indicated by changes in the intensity of this plane or screen of light. In particular, regions of vorticity will appear as small concentrated areas of limited light intensity.

The vapor-screen setup is shown schematically in figure 2. The photographs presented in this report were taken from a position upstream of the plane of light and encompass an area as shown in figure 2. In general, photographs of the flow were taken only over or close to the aft orifice station.

The tests were made in two series of runs. Vapor-screen tests, covering an angle-of-attack range from 0° to 34.5°, were first made on the ogive-cylinder configurations using a 20° bent sting. No pressure data were recorded, however, because an unsteady flow condition was not obtained. In an attempt to induce a fluctuating vortex motion the models were tested with and without axial transition strips (number 60 carborundum grains). In addition, the Reynolds number of the flow was varied from 1.73×10^6/ft to 4.94×10^6/ft.

The second series of tests were made using a 40° bent sting with a resulting angle-of-attack range from 17° to 50°. Pressure measurements and vapor-screen observations of the flow were made for the ogival, conical, and spike-tipped nose shapes. The Mach number of the tests was 2.01 and the Reynolds number per foot was 3.46×10^6. Tunnel stagnation conditions were as follows: temperature, 100° F; dewpoint (pressure runs), approximately -35° F; and pressure, 14.0 psia.

PRESENTATION AND DISCUSSION OF RESULTS

Vapor-screen photographs showing the flow characteristics near the base of each body are presented in figure 3 for various angles of attack. The static pressure distributions for the two body stations considered are presented in figure 4. No record of the instantaneous pressure variations (obtained from the electrical pressure pickups) are presented since a fluctuating or unsteady flow condition was not encountered except for one model configuration over a very limited angle range. In this

case the vortices in the field appeared to have no effect on the instantaneous body surface pressures.

The wake characteristics of the ogive-circular cylinder body are shown in figure 3(a). For angles of attack up to 34.5°, the wake pattern remained very steady and consisted of two symmetrically disposed vortices. Above an angle of attack of 35° the vortex pattern became asymmetrical and additional vortices appeared in the field. Although there was no indication of a rapid aperiodic switching of the vortices at the higher angles of attack, the vortex pattern did reverse between 40° and 45°. This phenomena appeared to be a smooth transition in which the vortices merged and then formed in a pattern opposite to that of the original configuration.

The wake patterns formed in the lee of the cone-circular cylinder body are shown in figure 3(b). Two major differences may be noted between the results for the ogive cylinder and the cone cylinder. First, the formation of an asymmetrical pattern occurred at a lower angle of attack with the conical nose shape; and second, the character of the wake was quite different between 40° and 50°. Although the vapor-screen tests of the cone cylinder body showed no flow asymmetry below an angle of about 25°, the pressure distributions (fig. 4(b)) indicate that some asymmetry existed at an angle of 17°, the minimum angle possible in this case. This difference may be attributed to the poor definition of the flow phenomena given by the vapor-screen technique at the lower angles of attack. As the angle of attack was increased beyond 40° the individual vortices appeared to lose strength and definition. At the maximum angle of 50° the flow was characterized in the vapor screen by a dark wake in which vortices were not discernible.

The wake characteristics of the spike-nosed circular-cylinder body, shown in figure 3(c), were somewhat similar in appearance to the conical-nosed body. In this case, however, an unsteady flow phenomena (i.e., a rapid aperiodic switching of the vortex pattern) was noted at an angle of attack of approximately 28°. This was a sharply tuned phenomena (occurring over an angle-of-attack range of less than 1°) which appeared to be an intermediate stage in the transition from a symmetrical to an asymmetrical distribution. Again, it should be noted that individual vortices were not discernible at the higher angles of attack.

Typical wake patterns in the lee of the elliptical body (major axis perpendicular to the cross flow) are shown in figures 3(d) and 3(e). As with the circular cylinder model, for the case of an ogival nose shape, an asymmetrical pattern did not develop until very high angles of attack were reached, in this case of the order of 40°. The use of a conical nose reduced this angle to a value between 25° and 30°. Although it is not apparent from the figure, the wake of the conical-nosed body at an angle of 50° was composed of a number of vortices which were

vibrating in unison towards and away from the model; however, no vortex switching was apparent.

The wake patterns for the ellipse with the minor axis perpendicular to the cross flow are shown in figure 3(f). The ogive nose-shape configuration only is presented since the vapor-screen photographs of the conical-nosed body were not very distinct. Essentially, however, the differences in the vortex patterns were similar to those exhibited by the circular cylinder body. The replacement of the ogive with the cone resulted in a more even distribution of vortices in the field for moderate angles and the disappearance of individual vortices at the higher angles of attack.

Although no vapor-screen photographs of the flow over the forward orifice station were obtained for any of the models, it is apparent from an examination of the body pressure distributions (fig. 4) that the asymmetrical flow pattern was reversed in some cases; i.e., the vortex closest to the body would be on one side of the model at the forward station and on the opposite side at the rearward station. For example, in figure 4(b), $\alpha = 28^\circ$, and in figure 4(g), $\alpha = 25^\circ$, it may be noted that the pressures on the leeward side of the model have opposite trends at the two longitudinal stations. From an examination of the schlieren photographs of reference 3 (figs. 8 and 9, specifically) it is apparent that the distribution of an asymmetrical vortex pattern is dependent upon the body station and that additional vortex cores appear in the field as the distance from the body nose is increased.

Perhaps the most unexpected result of the present investigation was the absence, except in one isolated case, of any unsteady vortex motion. This phenomena, noted in references 1 to 4, is a very rapid fluctuation or switching of the vortex pattern; i.e., the distribution of vortices at one instant of time would be completely reversed during the next instant of time. Thus, the vortex closest to the body would first appear on one side of the model and then on the other. This motion was entirely aperiodic and very pronounced in action. As stated previously, a similar phenomena was noted in the wake of the spike-nosed circular cylinder, although in this case it was not a definite body wake characteristic that existed over an appreciable angle-of-attack range.

In an attempt to excite or initiate a condition of vortex switching, full body-length axial transition strips (number 60 carborundum grains set in shellac) were added on the windward side of the ogive-cylinder bodies during the initial vapor-screen runs (α_{max} restricted to 34.5°). These strips were placed first at radial angles of 75° and 285°, and then at 65° and 295°. In addition, the free stream Reynolds number was varied from 1.73×10^6/ft to 4.94×10^6/ft. No data for this series of tests are presented, however, since no appreciable change in the character of the vortex pattern was noted. This result was observed in reference 2

where it was found that a change in Reynolds number had no effect on bodies with low fineness-ratio nose shapes. With an increase in nose fineness ratios, however, it was noted in reference 2 that an increase in Reynolds number resulted in a decrease in the angle at which an asymmetrical vortex pattern and subsequent flow unsteadiness occurred.

An explanation of the differences which exist between the results of this investigation and those reported in references 1 to 4 is not readily apparent since items such as tunnel turbulence levels, model mounting systems and model surface asymmetries may all be contributing factors. However, in light of the differences which do exist, it is apparent that additional investigations are needed before the exact properties of body vortex configurations may accurately be defined.

CONCLUDING REMARKS

An investigation has been made at a Mach number of 2.01 to study the flow in the lee of circular and elliptical cylinder bodies with both ogival and conical nose shapes. The characteristics of the wake vortex patterns near the base of each body were studied by means of the vapor-screen technique.

As the angle of attack was increased, the body wake patterns changed from a symmetrical pair of vortices to an asymmetrical distribution of two or more vortices. The angle at which an asymmetrical flow was first noted for any particular model configuration was dependent upon the body nose shape. The flow in the lee of the bodies with the fineness-ratio-3.5 ogival nose shape remained symmetrical to a much higher angle of attack than for the fineness-ratio-6 conical nose shape.

Although some wake vortex motion was apparent, a rapid aperiodic switiching of the vortex pattern was noted only for the spike-tipped circular cylinder model. This vortex switching did not exist over any appreciable angle-of-attack range. The conical nose shapes appeared to cause a deterioration of the vortex pattern above an angle of attack of 40° except for the elliptical body with the major axis perpendicular to the cross flow.

Langley Aeronautical Laboratory,
National Advisory Committee for Aeronautics,
Langley Field, Va., August 18, 1955.

REFERENCES

1. Mead, Merrill H.: Observations of Unsteady Flow Phenomena for an Inclinded Body Fitted With Stabilizing Fins. NACA RM A51K05, 1952.

2. Gowen, Forrest E., and Perkins, Edward W.: A Study of the Effects of Body Shape on the Vortex Wakes of Inclined Bodies at a Mach Number of 2. NACA RM A53I17, 1953.

3. Gowen, Forrest E.: Buffeting of a Vertical Tail on an Inclined Body at Supersonic Mach Numbers. NACA RM A53A09, 1953.

4. Seiff, Alvin, Sandahl, Carl A., Chapman, Dean R., Perkins, Edward W., and Gowen, F. E.: Aerodynamic Characteristics of Bodies at Supersonic Speeds. A Collection of Three Papers. NACA RM A51J25, 1951.

5. Allen, H. Julian, and Perkins, Edward W.: Characteristics of Flow Over Inclined Bodies of Revolution. NACA RM A50L07, 1951.

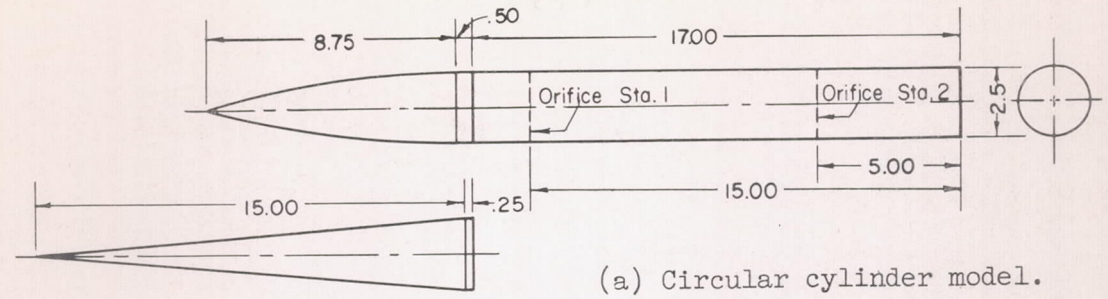

(a) Circular cylinder model.

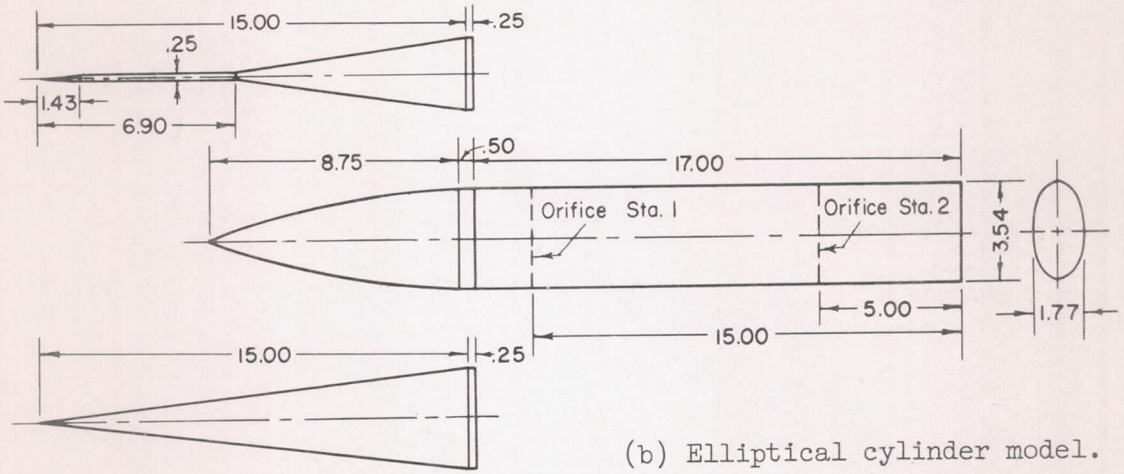

(b) Elliptical cylinder model.

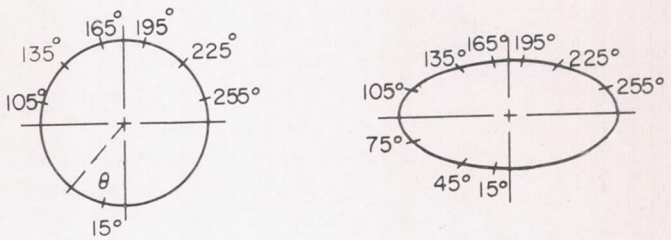

(c) Location of electrical pressure pickups.

Figure 1.- Schematic diagram of test models. (All dimensions are in inches unless otherwise specified.)

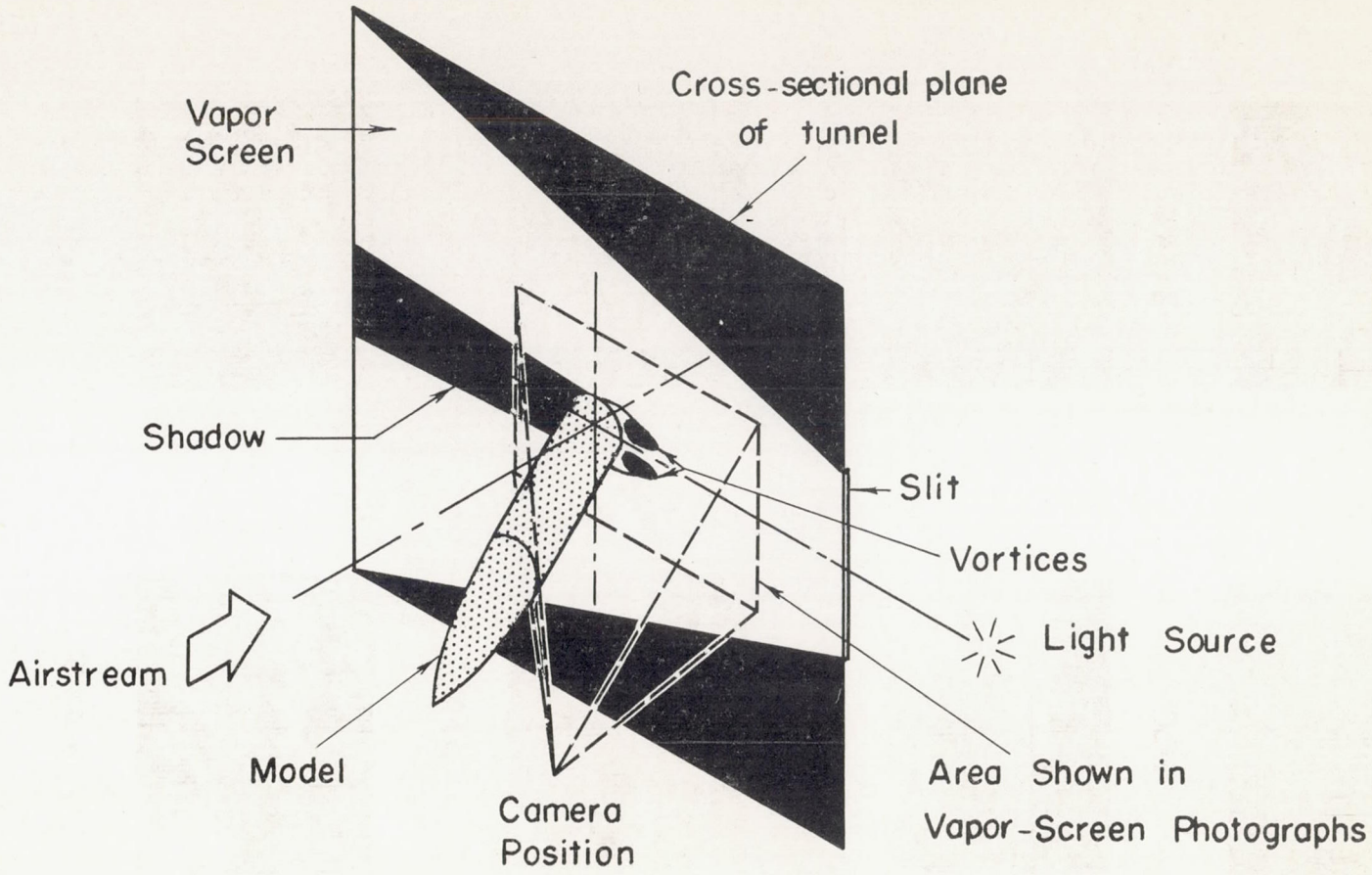

Figure 2.- Schematic diagram of vapor-screen setup.

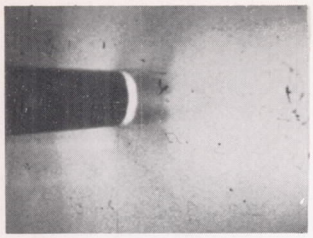

$\alpha = 30°$

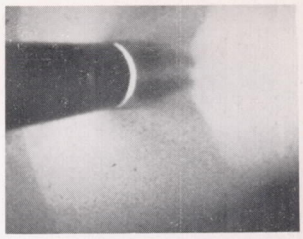

$\alpha = 34.5°$

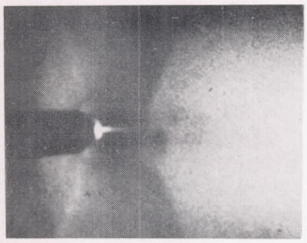

$\alpha = 35°$

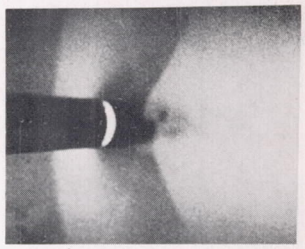

$\alpha = 37.5°$

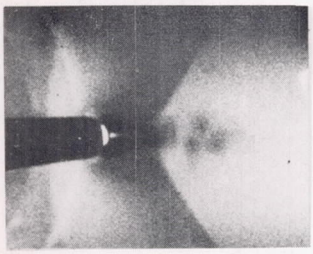

$\alpha = 39.3°$

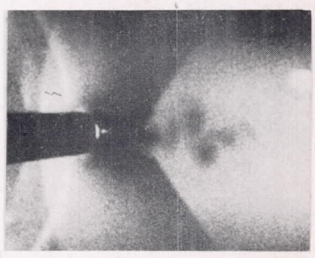

$\alpha = 41.1°$

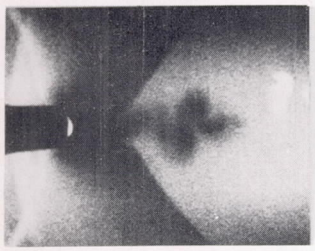

$\alpha = 44.8°$

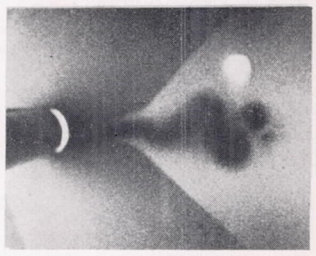

$\alpha = 50°$

(a) Ogive-circular cylinder.

L-90471

Figure 3.- Vapor-screen photographs of wake patterns in the lee of bodies at high angles of attack.

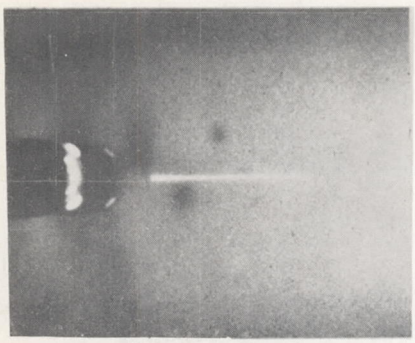

$\alpha = 30°$

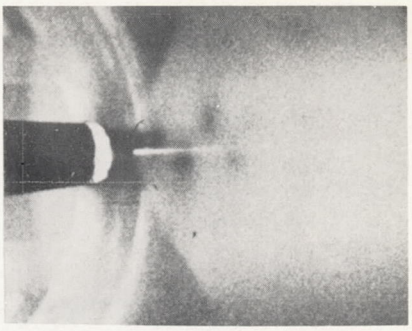

$\alpha = 35°$

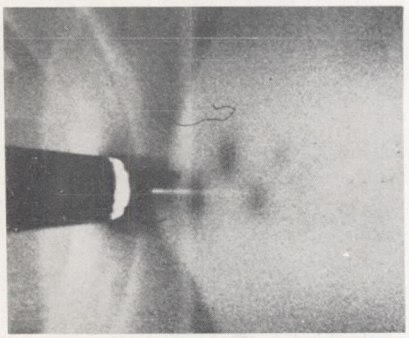

$\alpha = 36°$

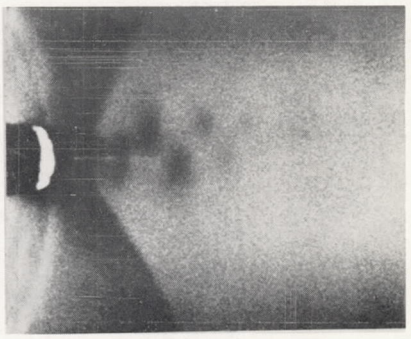

$\alpha = 39°$

$\alpha = 41°$

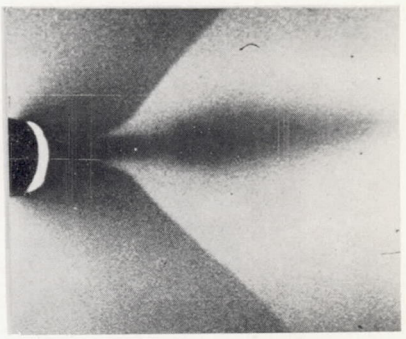

$\alpha = 50°$

L-90472

(b) Cone-circular cylinder.

Figure 3.- Continued.

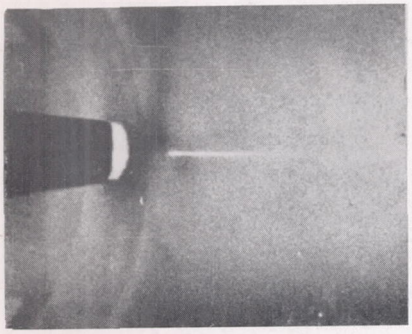

$\alpha \cong 28°$

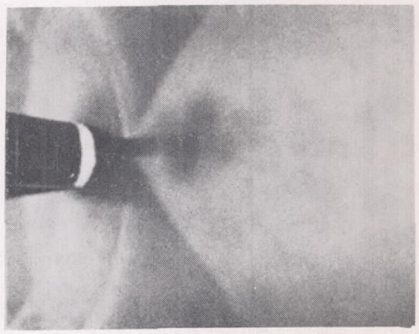

$\alpha \cong 40°$

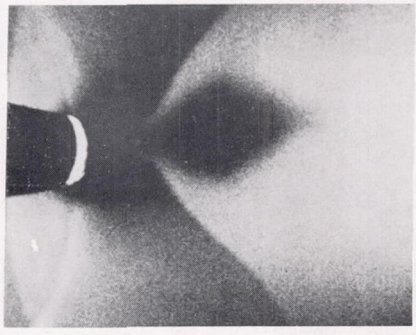

$\alpha = 50°$

L-90473

(c) Spike-nosed circular cylinder.

Figure 3.- Continued.

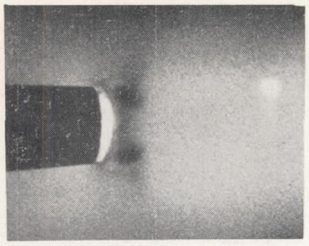

$\alpha = 20°$

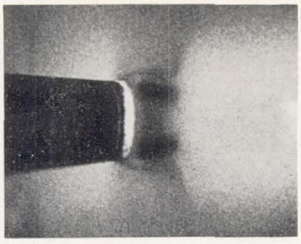

$\alpha = 25°$

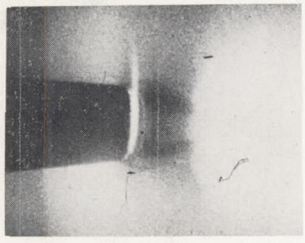

$\alpha = 30°$

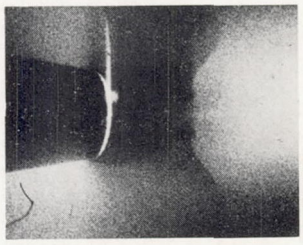

$\alpha = 34.5°$

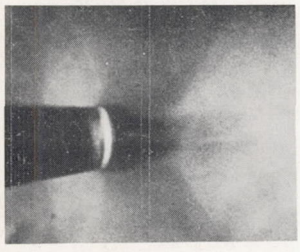

$\alpha = 40°$

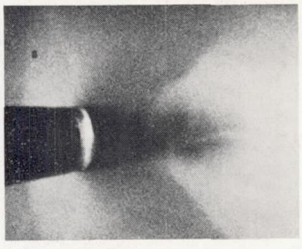

$\alpha = 45°$

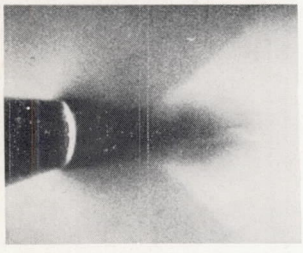

$\alpha = 48.5°$

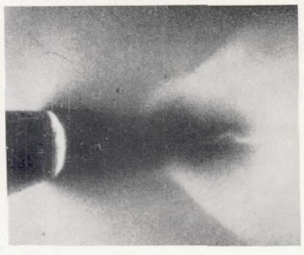

$\alpha = 50°$

L-90474

(d) Ogive-elliptical cylinder. Major axis perpendicular to cross flow.

Figure 3.- Continued.

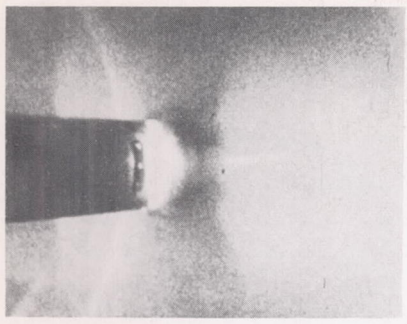

$\alpha = 25°$

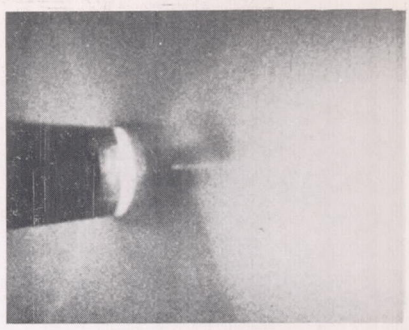

$\alpha = 30°$

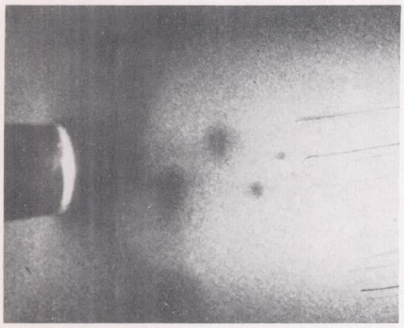

$\alpha = 35°$

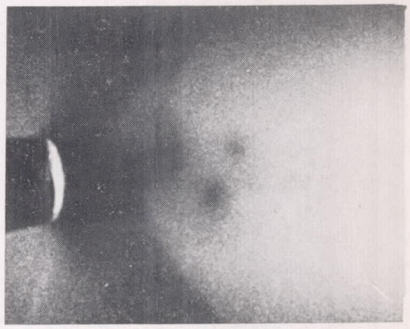

$\alpha = 40°$

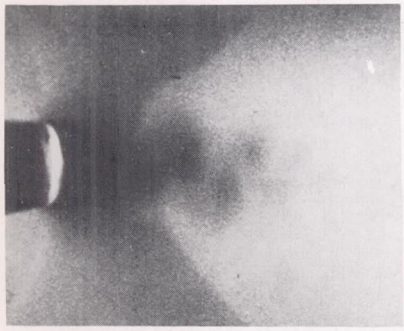

$\alpha = 45°$

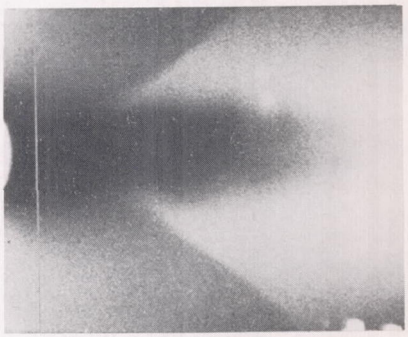

$\alpha = 50°$

L-90475

(e) Cone-elliptical cylinder. Major axis perpendicular to cross flow.

Figure 3.- Continued.

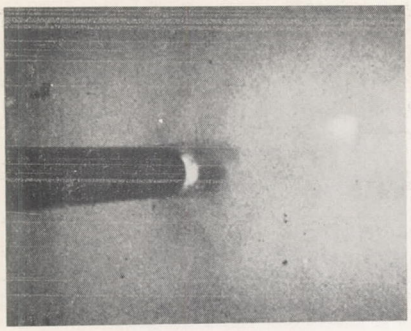

$\alpha = 25°$

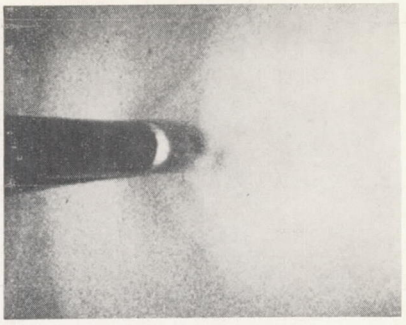

$\alpha = 30°$

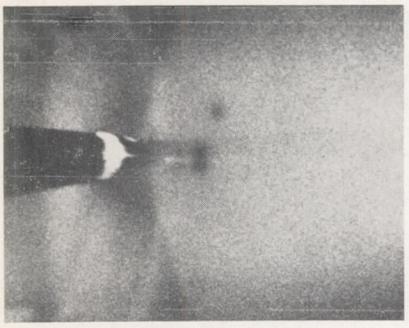

$\alpha = 35°$

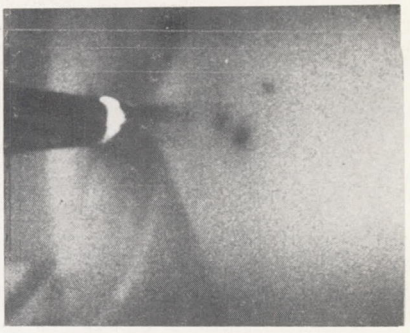

$\alpha = 40°$

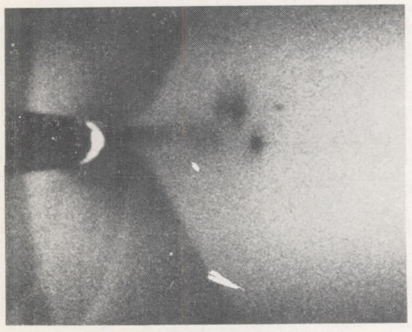

$\alpha = 45°$

$\alpha = 50°$

L-90476

(f) Ogive-elliptical cylinder. Minor axis perpendicular to cross flow.

Figure 3.- Concluded.

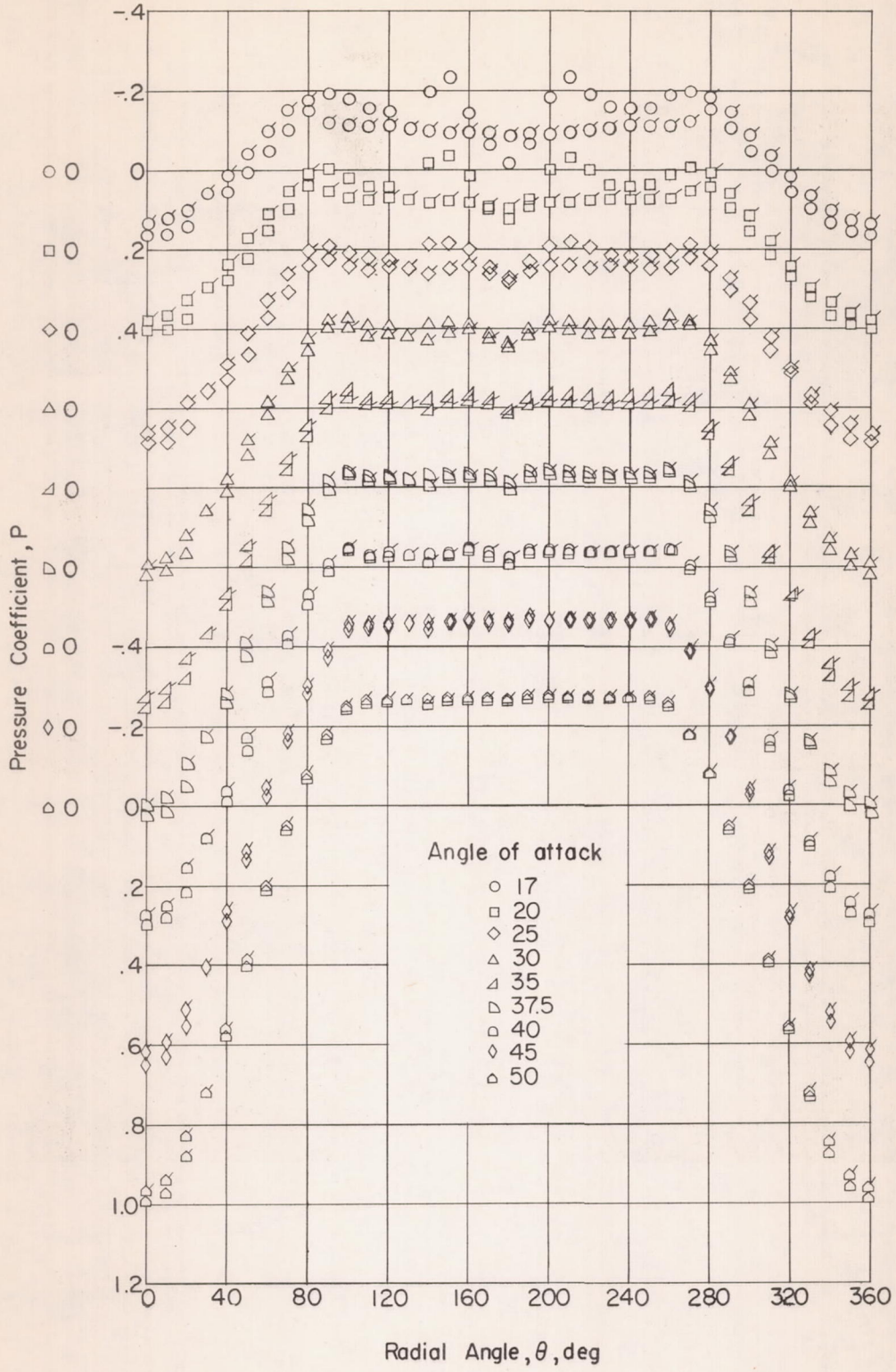

(a) Ogive-circular cylinder.

Figure 4.- Variation with radial angle of the pressure coefficient at two longitudinal body stations. Plain symbols denote station 1; flagged symbols denote station 2.

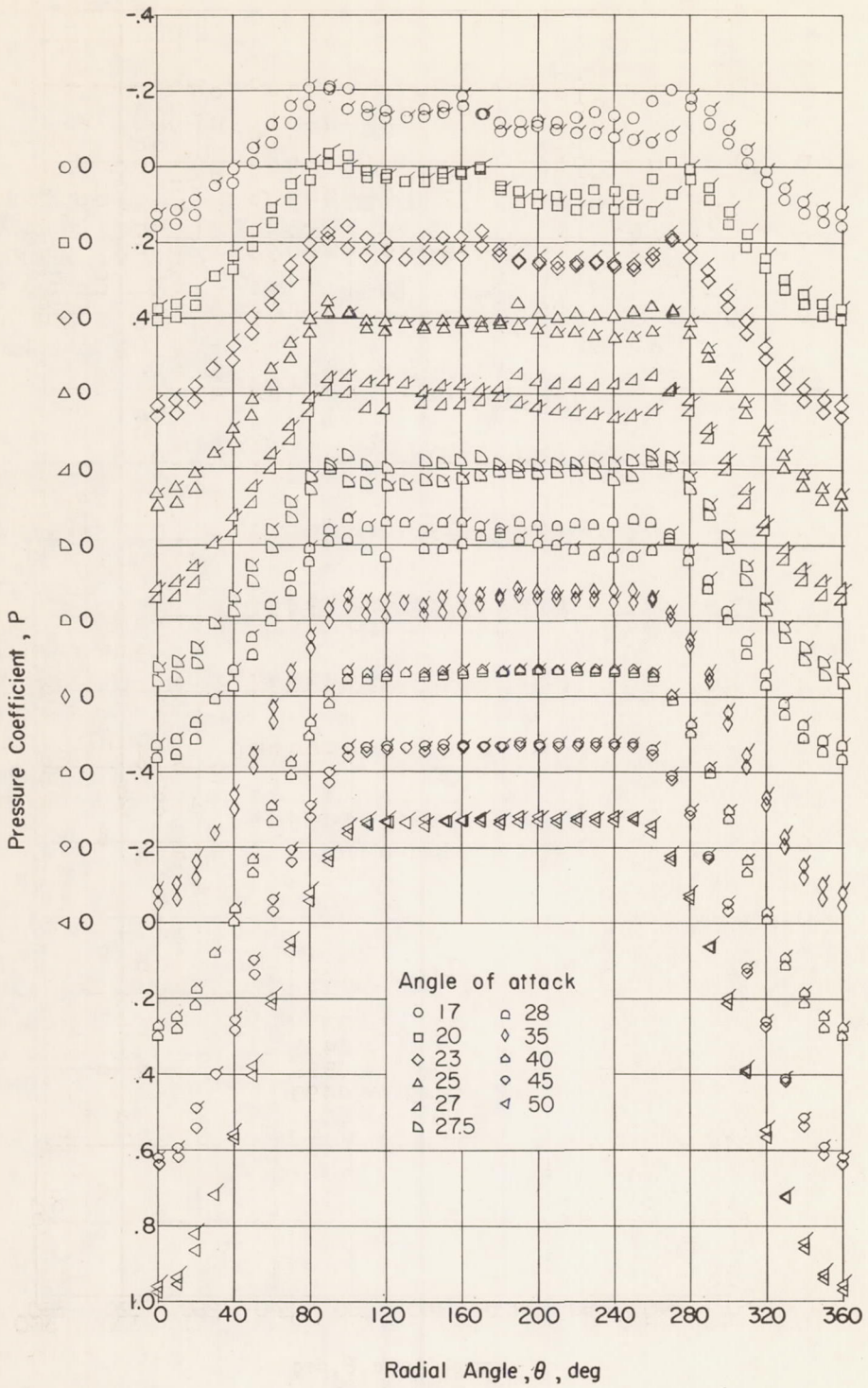

(b) Cone-circular cylinder.

Figure 4.- Continued.

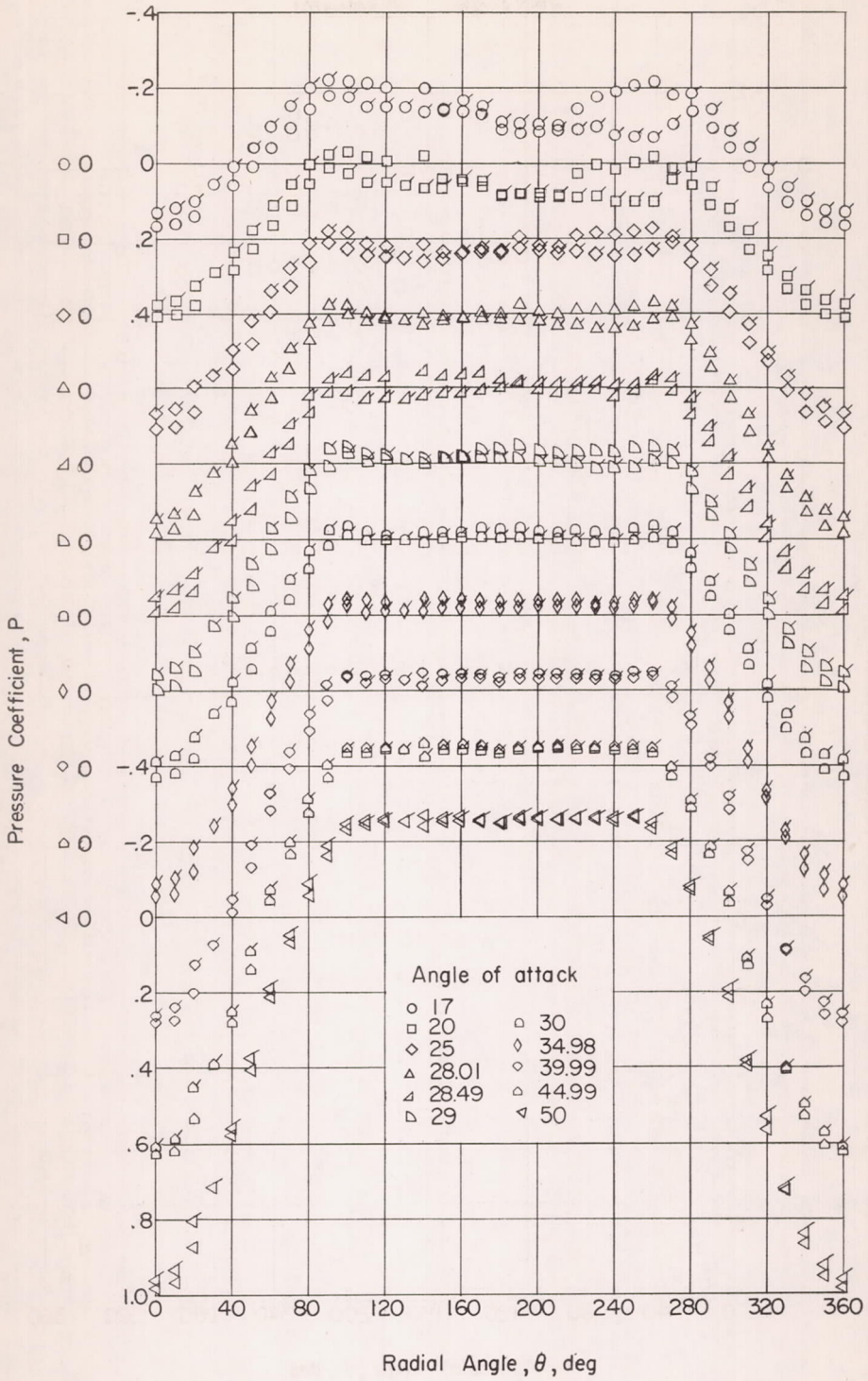

(c) Spike-nosed circular cylinder.

Figure 4.- Continued.

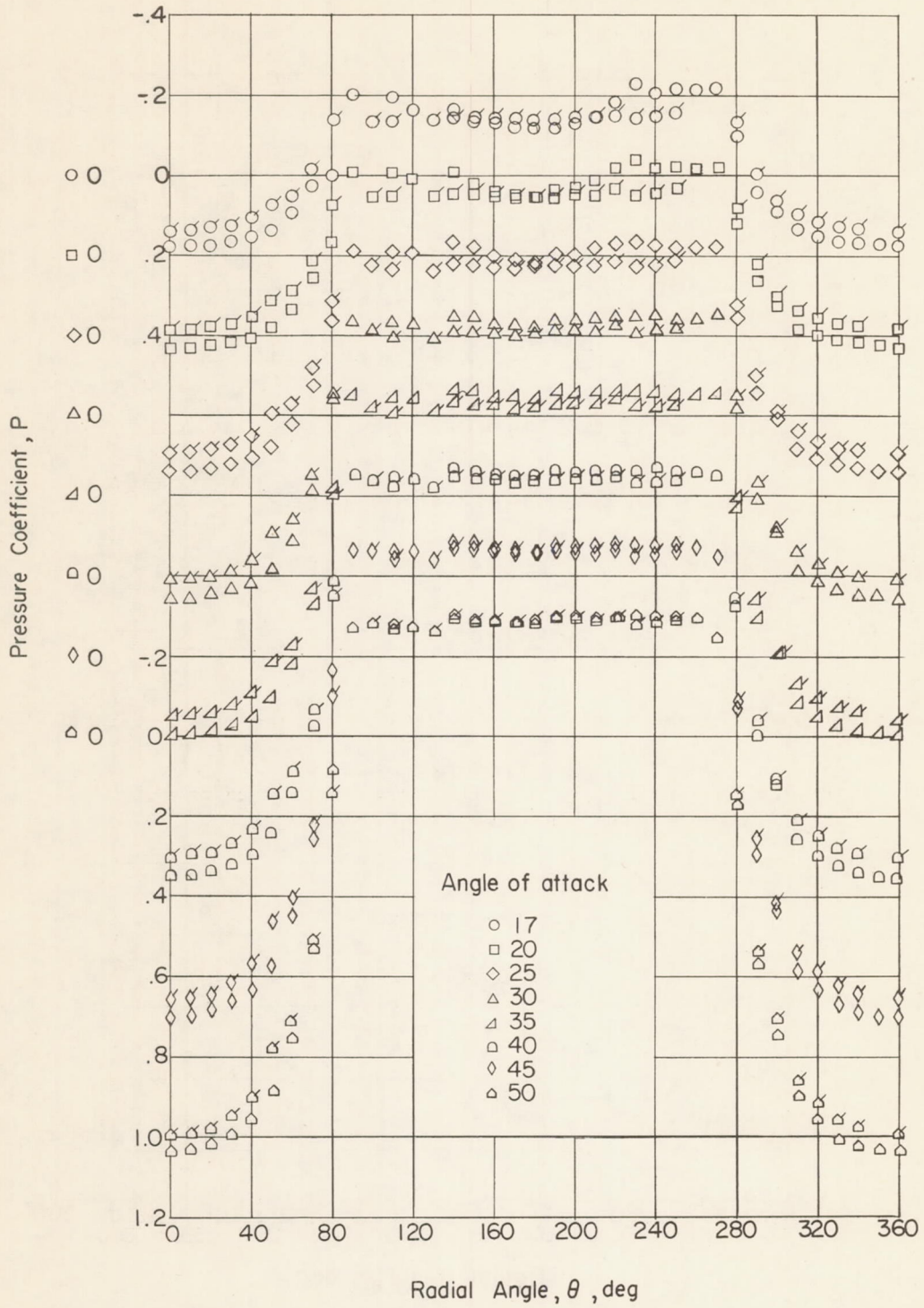

(d) Ogive-elliptical cylinder. Major axis perpendicular to cross flow.

Figure 4.- Continued.

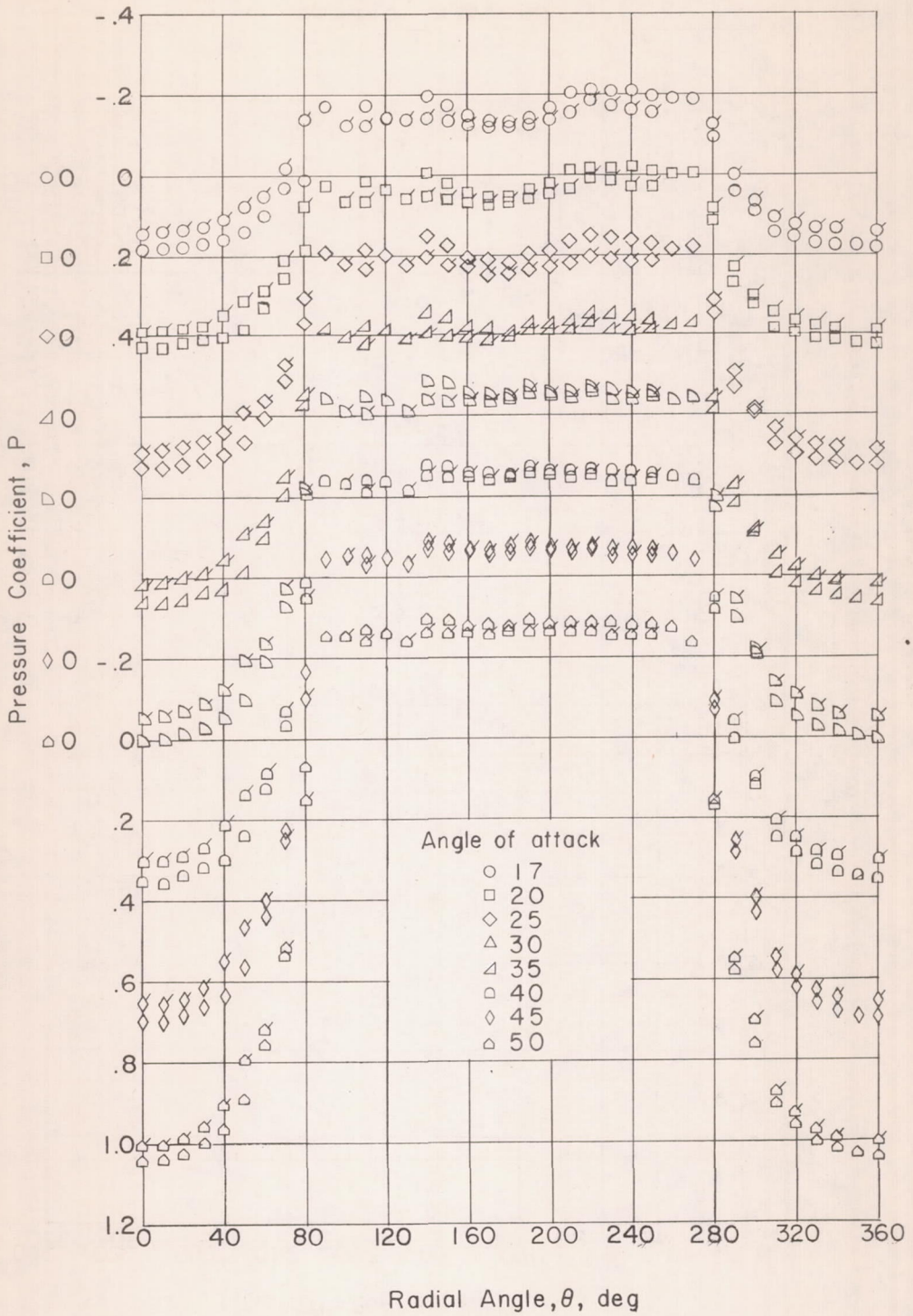

(e) Cone-elliptical cylinder. Major axis perpendicular to cross flow.

Figure 4.- Continued.

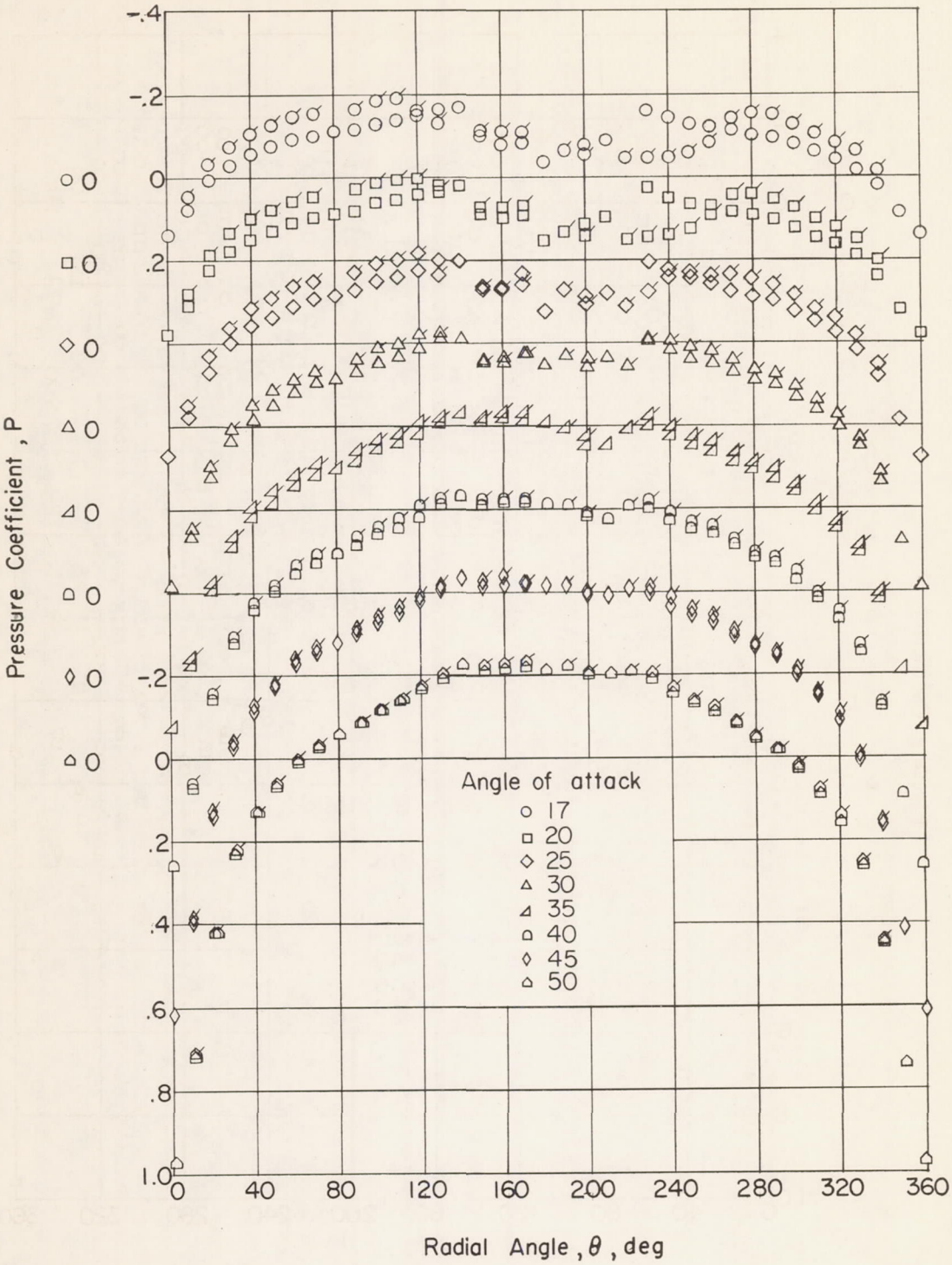

(f) Ogive-elliptical cylinder. Minor axis perpendicular to cross flow.

Figure 4.- Continued.

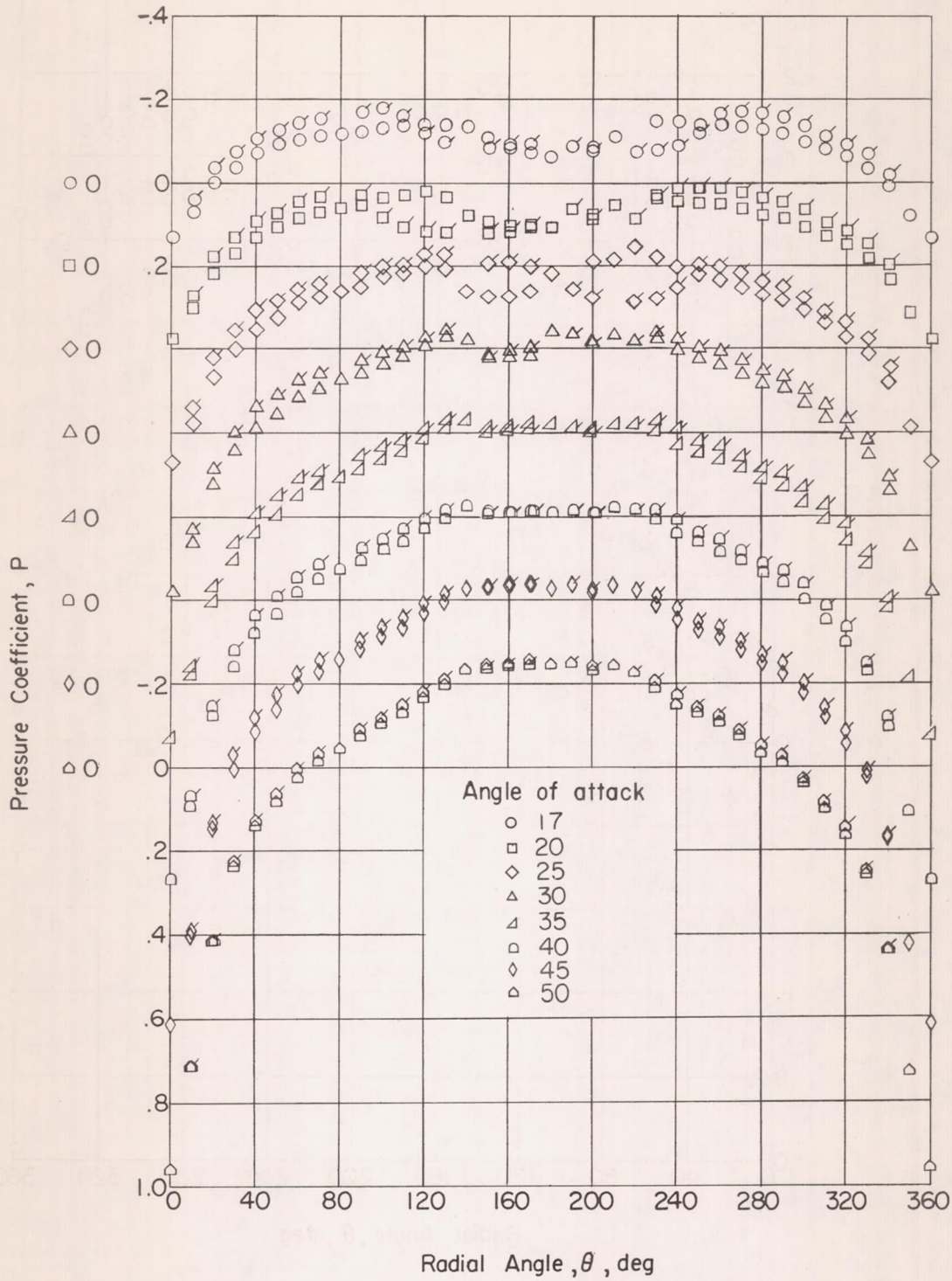

(g) Cone-elliptical cylinder. Minor axis perpendicular to cross flow.

Figure 4.- Concluded.